Energy Reports 13 (2025) 642–652

Contents lists available at ScienceDirect

Energy Reports

journal homepage: www.elsevier.com/locate/egyr

Research paper

# Quantification of the impact of irradiance, heat, humidity, and cyclic temperature on the aging of photovoltaic panels: a case study in Algeria

Meriem Farou [a,b,*], Abdelhak Djellad [a,b], Sofiane Chiheb [a,b], Hala Lalaymia [a,b], Badri Rekik [a,b], Pierre-Olivier Logerais [c]

[a] National Higher School of Technology and Engineering, Department of Electronics, Electrical Engineering and Automation, Annaba, 23005, Sidi Amar, Algeria
[b] Laboratory of Technologies of Energetic Systems E3360100, National Higher School of Technology and Engineering, Annaba, 23005, Sidi Amar, Algeria
[c] Univ. Paris-Est Créteil, 61avenue du Général de Gaulle, Paris, F-94010, Créteil, France

ARTICLE INFO

*Keywords:*
Photovoltaic
Degradation
Aging
Accelerated lifetime

ABSTRACT

Photovoltaic (PV) aging refers to the inevitable decline in the efficiency of solar modules over time due to various environmental factors. The main elements contributing to this degradation include irradiance, heat, humidity, and cyclic temperature. This paper details the accelerated factors (AFs) calculated from a series of developed equations established to quantify the deterioration mechanisms affecting PV panels. These equations are derived from several models: the Arrhenius model for temperature and irradiance, the Eyring and Peck models for humidity, and the Coffin-Manson model for cyclic temperature. After formulating equations that measure the combined effects of temperature, irradiance, humidity, and cyclic temperature, these equations were employed to analyze the deterioration of the PV panels installed at the Oued El Keberit solar plant in Souk Ahras, Algeria. The investigation revealed that humidity significantly affected the panels during the winter season. In spring, both humidity and irradiance become important factors. During the summer, temperature greatly influences degradation, while lower humidity levels do not significantly affect the panels. In autumn, humidity continues to be a critical factor. According to the obtained results, the highest AF values occur during the summer months, while the lowest AF values are observed in winter. As a result, the PV panels would deteriorate more noticeably during the winter season than in the summer time.

## 1. Introduction

The accelerated use of conventional energy resources, such as fossil fuels, driven by the world's population and economic growth, has had a detrimental effect on the environment. Furthermore, at the current rate of energy demand, fossil fuels will eventually run out of stock (Liu et al., 2024). Photovoltaic (PV) solar cells are indeed a significant player in the realm of renewable energy sources, showcasing the immense potential to meet future energy demands (Yekinni et al., 2023). PV cells are the primary components for converting solar radiation into electricity, contributing to the overall energy efficiency of PV power plants (Torlo et al., 2023). While solar energy is a reliable renewable source, its limitations, such as weather dependency and daytime availability, can be mitigated by connecting solar power systems to the grid for a more balanced energy supply (Mistry et al., 2022). The broader scope of renewable energy includes various sources like wind and solar power, with advancements in these technologies leading to decreased costs and increased global capacity for renewable energy generation (Talib, 2022). Evidence suggests that solar systems possess an extended lifespan. Nevertheless, the systems experience a progressive decline in efficiency (Gopinath and Marimuthu, 2024). The aging of PV modules can be modeled through simulated electrical characteristics, with a focus on factors like optical transmittance and electrical degradations, leading to a power degradation rate of around 0.53% per year (Doumane et al., 2015). Additionally, understanding the processes of photochemical aging and weathering is essential to prevent degradation reactions in polymeric materials exposed to solar radiation, particularly in the UV range (Feil et al., 2022). Evaluating the stress variables that affect PV modules and establishing a correlation with their response is essential for comprehending their long-term performance. These stress parameters are accountable for deciding the deterioration of the components, and as a result, their lifespan (Alavi et al., 2024).

Irradiance significantly impacts the performance of PV modules. Studies have shown that the degradation rates of polycrystalline PV panels can significantly increase under different irradiance levels, with average degradation rates of 1.02%/year at 800 $W/m^2$ and 0.99%/year

* Correspondence to: Cité UV2, Building 2L, Block 1, Door Number 9, Sidi Amar, Annaba, Algeria.
*E-mail address:* m.farou@etu.ensti-annaba.dz (M. Farou).

https://doi.org/10.1016/j.egyr.2024.12.025
Received 1 August 2024; Received in revised form 10 November 2024; Accepted 9 December 2024
Available online 20 December 2024
2352-4847/© 2024 The Authors. Published by Elsevier Ltd. This is an open access article under the CC BY-NC license (http://creativecommons.org/licenses/by-nc/4.0/).

at 600 W/m$^2$, exceeding manufacturer-proposed values (Shaik et al., 2021). Other types of panels are also subject to degradation at comparable rates: 1.50% per year for amorphous silicon (a-Si) panels, 0.92% per year for Copper Indium Gallium Selenide (CIGS) panels, and 0.62% per year for Cadmium Telluride (CdTe) panels (Solís-Alemán et al., 2019). Accelerated lifetime testing labs have been established to assess material reliability under varying irradiance conditions, with precise control of sample temperatures and irradiances to study degradation kinetics under high-concentration conditions (Burlafinger, 2020). In addition, the correlation between irradiance data collection locations and module performance has been found to impact the accuracy of irradiance-to-power models, with site-specific data coupled with accelerated lifecycle testing improving power predictions (Dzurick et al., 2019). Furthermore, the degradation of the ethylene-vinyl acetate (EVA) encapsulant due to prolonged ultraviolet exposure and other environmental stress factors can lead to significant power loss, emphasizing the importance of predicting EVA degradation through short-circuit current evaluations (Mahdi et al., 2021). A method to report PV system degradation rates without irradiance data has also been demonstrated, showcasing the potential for alternative approaches in degradation studies (Cronin et al., 2014).

Equally important is the role of temperature in the degradation of PV modules. Research indicates that elevated temperatures can lead to potential induced degradation (PID) in multicrystalline silicon (mc-Si) PV solar panels, causing substantial power loss due to large leakage currents and negative temperature coefficients of key parameters like the open-circuit voltage $\beta_{V_{OC}} = -0.4\% /°C$, the voltage at the maximum power point $\beta_{V_{mpp}} = -0.5\% /°C$, and the fill factor $\beta_{FF} = -0.2\% /°C$ (Segbefia and Sætre, 2022). Comprehending the thermal dynamics of silicon photovoltaic (Si PV) devices is crucial, especially during the summer months in desert regions, such as Colorado. This analysis indicates that under extreme conditions, with minimal convective heat transfer, the photo-absorber temperature can reach around 82 °C. The c-Si device exhibits a power loss rate of 0.45%/°C, translated to approximately 200 mV loss at 70 °C, given that the power degradation is directly linked to the increase in temperature and its impact on the output voltage of the device (Bae et al., 2020). And over, studies on silicon heterojunction (SHJ) PV modules show that higher temperatures during PID tests result in a faster decrease in the short-circuit current density (Jsc), which can be mitigated by pre-annealing at high temperatures (Xu et al., 2022). Furthermore, light- and elevated-temperature-induced degradation (LeTID) in monocrystalline silicon cells is linked to a majority-carrier hole-trap defects with specific activation energies and trap densities, highlighting the impact of temperature on the performance of PV modules (Johnston et al., 2022; Karas et al., 2023). Understanding these temperature-induced degradation mechanisms is essential for improving the durability and efficiency of solar energy systems.

Moreover, humidity must be taken into account as it significantly contributes to the deterioration of PV modules and affects their performance over time. Studies have shown that in tropical areas characterized by high heat and humidity, the electrical parameters of PV panels degrade, leading to performance losses (Capo-Chichi et al., 2022). Moisture, particularly in the form of humidity, can accelerate degradation processes in PV modules, causing a decrease in key electrical parameters such as Fill Factor and Power Conversion Efficiency (Yao et al., 2022). Additionally, the sensitivity of all-inorganic perovskites to environmental factors like relative humidity can lead to degradation mechanisms that affect the PV performance of solar cells (Mohamed et al., 2017). Besides, potential-induced degradation in PV panels is influenced by humidity levels, with higher humidity leading to increased leakage currents and accelerated stress on the modules (Kyranaki et al., 2022). Understanding and mitigating the impact of humidity on PV degradation is important for improving the long-term performance and reliability of solar energy systems.

Another critical factor is the cyclic temperature fluctuations, which significantly affect PV degradation. These repeated temperature fluctuations can cause stress on PV materials, leading to microcracks, delamination, and other forms of mechanical and chemical degradation over time. Among these, delamination is one of the most well-recognized and critical degradation mechanisms in PV modules. It occurs when the encapsulant, such as EVA, loses adhesion to adjacent layers, often as a result of prolonged exposure to environmental stressors like temperature variations and humidity. This loss of adhesion compromises the structural integrity of the module, leading to a decline in performance and lifespan. Fig. 1 illustrates the delamination process using supercritical $CO_2$, where the absorption of $CO_2$ and the subsequent foaming effect generate mechanical stresses that separate the encapsulant from the glass and backsheet layers. While this process contributes to the degradation of active PV modules, it is also employed as an efficient recycling technique, enabling the recovery of valuable materials from the end-of-life of PV systems (Briand et al., 2023). As studied in various research papers, cyclic temperature PV degradation involves exposing solar modules to temperature cycles to simulate natural conditions and assess their reliability. As studied in various research papers, cyclic temperature PV degradation involves exposing solar modules to temperature cycling to simulate natural conditions and assess their reliability. The degradation mechanisms identified include an increase in the series resistance due to the loss of pressure contact, a rise in the aluminum sheet resistance, and in the solder contact resistance (Urban et al., 2022). Different behaviors are observed in P-mono and P-multi PV modules after temperature cycling, with recovery effects noted in pre-conditioned P-mono modules (Chen et al., 2014). Factors contributing to degradation include temperature, moisture, ultraviolet radiation, and negative bias voltage, affecting polymeric and metallic components of the modules (Koehl et al., 2017). Temperature-cycling tests, such as those specified in IEC standards, induce stress at material interfaces, particularly affecting cell connectors and leading to material fatigue (Herrmann, 2010). Accelerated thermal cycling tests show variable performances among PV modules when new, with power reduction ranging from 1.4% to 7.6% after degradation, as demonstrated by Electrochemical Impedance Spectroscopy analysis (Perez et al., 2019).

This study quantifies the accelerated factors (AFs) by simultaneously incorporating four key environmental parameters: irradiance, temperature, relative humidity, and cyclic temperature (see Fig. 2). Unlike prior studies that may have focused on these factors individually or in partial combinations, this work is the first to employ multiple models combined: Arrhenius for temperature and irradiance, Eyring and Peck for humidity, and Coffin–Manson for cyclic temperature together in a comprehensive assessment. The investigation, conducted here for the case of the location of a PV plant in Algeria, allows for an evaluation of how local climatic variations affect the performance of PV panels. The structure of the paper is as follows: Section 2 presents the equations and models employed for calculating the AFs of PV modules, while Section 3 offers a thorough analysis of the results, supported by detailed figures and tables displaying the computed AF values. The paper concludes with a discussion of the findings and outlines perspectives for future research and applications.

## 2. Calculation models employed for AFs

The foundation of accelerated aging processes relies on models that elucidate the relationship between aging and various environmental factors. These models are crucial for predicting the lifespan of materials and electronics, anticipating their performance degradation across different environmental conditions, and assessing their economic viability (Pramanick and Kumar, 2024). Acceleration models commonly employed are the Arrhenius, inverse power, Peck, Eyring, Zhurkov, and polynomial models. The Arrhenius model is frequently employed as an acceleration model when temperature serves as the acceleration stress (Hulkoff, 2009). The Zhurkov model, on the other hand, can be utilized for both temperature and mechanical stress. Lastly, the Peck

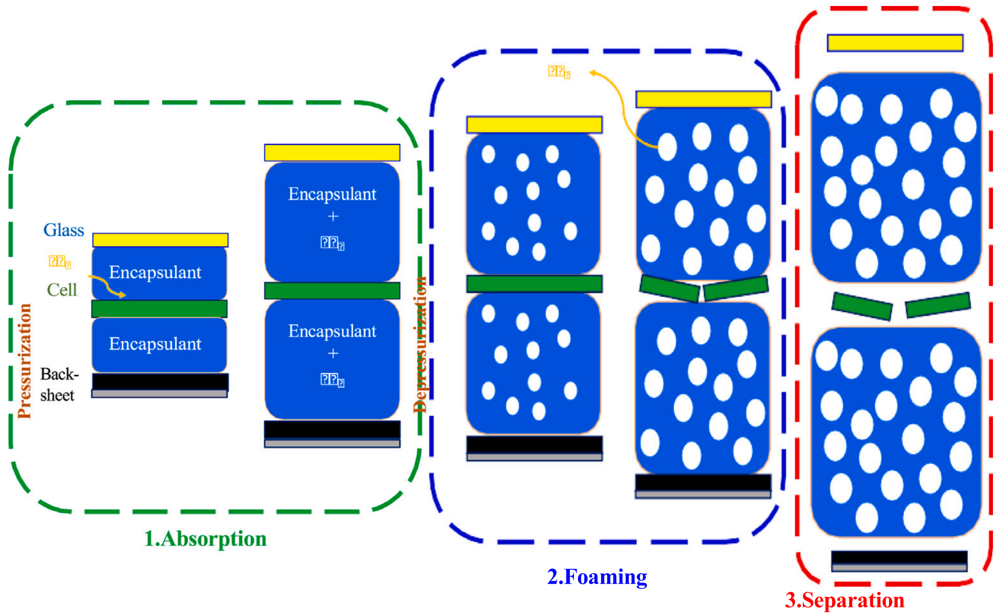


**Fig. 1.** Schematic representation of the different stages in the supercritical $CO_2$ delamination process (Briand et al., 2023).

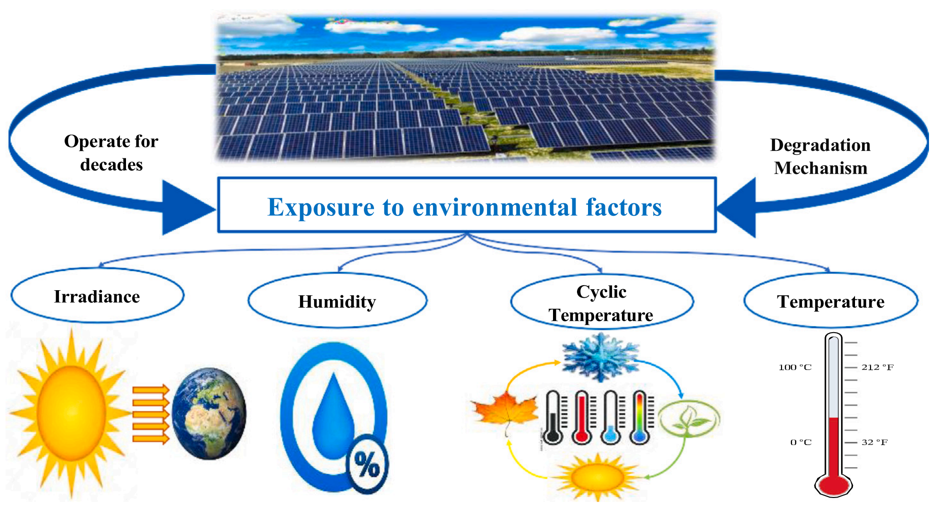


**Fig. 2.** Environmental factors that accelerate the aging of PV modules.

model is employed when considering temperature and humidity (Liu et al., 2019). This research employed the Arrhenius model to develop an acceleration model based on both temperature and irradiance, effectively illustrating how these two factors influence the degradation of PV panels. Grounded on kinetic theory, the Arrhenius model elucidates how temperature affects the rate of chemical reactions by postulating that higher temperatures increase molecular movement, leading to more frequent collisions and accelerated degradation processes. In addition, the Peck and Eyring models were utilized to assess the effects of relative humidity on the aging process of PV panels. These models are essential, as they account for the significant role humidity plays in intensifying damage, an effect overlooked by the Arrhenius model. Furthermore, this study introduces the calculation of AFs for cyclic temperatures based on the Coffin-Manson approach. This method is also particularly relevant for understanding how materials respond to repeated temperature fluctuations, which is critical for solar modules subjected to varying environmental conditions over time. This aspect represents a significant contribution to the existing literature, as it has not been previously addressed, particularly when considering the combined influences of temperature, irradiation, and relative humidity. By integrating these critical factors, this work enhances the understanding of the degradation processes affecting PV panels under natural conditions, thereby improving predictive modeling and performance assessments.

### 2.1. Arrhenius model

The Arrhenius model is often employed to describe the relationship between temperature $T$ and the rate $k$ of chemical reactions (Çolak, 2022; Zang et al., 2023; Lugt, 2023) as defined in Eq. (1) (Kurtz et al., 2024; Tawagi et al., 2023). This model is a useful tool for scientists and engineers to understand temperature relationships, optimize processes, create materials specifically for applications, and predict how different systems would behave and hold up over time under various operating conditions (Sarma et al., 2024). The reaction rate k is expressed as:

$$k = \gamma e^{\frac{-E_a}{R_1 . T}} \tag{1}$$

where $\gamma$, $E_a$, $R_1$, and $T$ are the pre-exponential factor, the activation energy J/mol, the universal gas constant taken as 8.314 J mol$^{-1}$ K$^{-1}$, and the absolute temperature in Kelvin respectively. To determine a notable rate of deterioration under operational circumstances $k_{site}$ derived from the stressed-out accelerated degradation $k_{lab}$ rate, the accelerated factor $AF$ is as follows (Zhao et al., 2022; Damo et al., 2023):

$$AF = \frac{k_{lab}}{k_{site}} \tag{2}$$

#### 2.1.1. Accelerated factor of static panel temperature

The temperature of PV modules significantly limits their power output due to the negative temperature coefficient of the voltage of the modules. As the temperature rises, the voltage decreases, resulting in reduced voltage of the modules (Kidegho et al., 2021). The panel backsheet temperature is defined by the following equation (Damo et al., 2023):

$$T_{panel} = (G.e^{a+bv}) + T_{amb} \tag{3}$$

Where $G$, $v$, and $T_{amb}$ are the incident solar irradiance in $\mathrm{w/m^2}$, the wind speed in m/s and the ambient temperature respectively; $a$ and $b$ coefficients which are determined empirically and vary depending on the panel type (GCG: glass/cell/glass) or (GCP: glass/cell/back sheet) and the mounting configuration (open or closed rack). For the GCP configuration, the coefficients $a$ and $b$ are: −3.56 and −0.075 s/m respectively, while for the GCG configuration, $a$ is −3.47 and $b$ is −0.0594 s/m (Damo et al., 2023).

$T_{panel}$ is used to compute the cell temperature $T_{cell}$, through:

$$T_{cell} = T_{panel} + (\frac{G}{G_0}.\sigma T) \tag{4}$$

In Eq. (4), $G$ is the daily irradiance, $G_0$ is the reference irradiance taken as $1000\ \mathrm{w/m^2}$, and $\sigma T$ denotes the temperature gradient, which is 3 °C (Damo et al., 2023). After determining the cell temperature, we can introduce the accelerated factor below:

$$AF_T = \frac{k_{deg}(T_{lab})}{k_{deg}(T_{site})} = e^{\frac{-E_a}{R_1}.(\frac{1}{T_{lab}} - \frac{1}{T_{site}})} \tag{5}$$

Based on previous research (Damo et al., 2023), the activation energy $E_a$ can take according to the severity of environmental conditions and the robustness of the PV modules the values of: 34 kJ/mol, 42 kJ/mol, and 50.1 kJ/mol. $T_{site}$ is derived from $T_{eff}$, which is defined in Eq. (8). In contrast, $T_{lab}$ is assumed to be 85 °C.

### 2.2. Accelerated factor of static module temperature and irradiance

Exposure to sunlight leads to a deterioration process in the PV module caused by the combined effects of irradiance and temperature. The Arrhenius equation has to be adjusted to incorporate the impact of irradiance. The $AF_{T,G}$ can be obtained by multiplying $AF_T$ by $AF_G$ as defined in Eq. (6).

$$AF_{T,G} = AF_T.AF_G = \frac{k_{deg}(T,G)_{lab}}{k_{deg}(T,G)_{site}} = \frac{G_{lab}}{G_{site}}.e^{\frac{-E_a}{R_1}.(\frac{1}{T_{lab}} - \frac{1}{T_{site}})} \tag{6}$$

$G_{site}$ is the weighted average solar irradiance in the area where the PV module is being operated; $G_{lab}$ is set to $1000\ \mathrm{W/m^2}$. The calculation of the weighted average solar irradiance is done using:

$$G = \frac{\sum_i G_i.(\delta t)_i}{\sum_i(\delta t)_i} \tag{7}$$

$G_i$ is the average irradiance for the day or month and $\delta t_i$ is the number of seconds in the $i$th day or month.

A constant named effective temperature $T_{eff}$ has been introduced to account for fluctuations in irradiance and temperature in outdoor conditions. When considering temperature and irradiance alone, $T_{eff}$ is as follows (Damo et al., 2023):

$$T_{eff} = \frac{E_a}{R_1\ \log_e(\frac{\sum_i G_i.e^{\left(\frac{E_a}{R_1 T_i}\right)}(\delta t)_i}{\sum_t G_t.(\delta t)_t})} \tag{8}$$

$T_i$ refers to the cell temperature $T_{\mathrm{cell}}$, as specified in Eq. (4).

### 2.3. Accelerated factor of static module temperature, irradiance and cyclic temperature

#### 2.3.1. Coffin–manson model

The Coffin–Manson model has been employed for the purpose of predicting mechanical failure, material fatigue, and material deformation (Dalton et al., 2018). This model establishes a correlation between the lifespan of a product and the temperature cycles it experiences (Wang and Tang, 2020). The number of cycles to failure $N$ is introduced as follows (Bala Subramaniyan et al., 2018):

$$N = \frac{\gamma}{(\Delta T)^{\alpha}} \tag{9}$$

where $\Delta T$ is the cyclic temperature in Kelvin and $\alpha$ is a constant based on product characteristics, as determined by a study conducted by Bala Subramaniyan et al. (2018), and according to their findings, $\alpha$ can take on three values: a lower bound $\alpha_1 = 2.34$, an estimated $\alpha_2 = 2.41$, and an upper bound $\alpha_3 = 2.46$. These values are derived from a combination of empirical data analysis and statistical modeling, reflecting the degradation behavior of PV modules under varying environmental conditions. Thus, the accelerated factor for cyclic temperature $AF_{\Delta T}$, based on the Coffin–Manson model, is given in Eq. (10) (Escobar and Meeker, 2006).

$$AF_{\Delta T} = \left(\frac{\Delta T_{lab}}{\Delta T_{site}}\right)^{\alpha} \tag{10}$$

$\Delta T_{lab}$ is the temperature below which thermal cycling causes little or no fatigue damage (Escobar and Meeker, 2006), and $\Delta T_{site}$ is the cyclic temperature where the PV panel is used. The combined effect of temperature, irradiance and cyclic temperature is defined by:

$$AF_{T,G,\Delta T} = \frac{G_{lab}}{G_{site}}.\left(\frac{\Delta T_{lab}}{\Delta T_{site}}\right)^{\alpha}.e^{\frac{-E_a}{R_1}.(\frac{1}{T_{lab}} - \frac{1}{T_{site}})} \tag{11}$$

### 2.4. Accelerated factor of static module temperature, irradiance and relative humidity

#### 2.4.1. Peck model

Peck's equation, traditionally used to translate Highly Accelerated Stress Test (HAST) failure rates to application-specific conditions, faces challenges in accurately projecting lifetime due to the correlation between relative humidity (RH) and temperature in self-heated Integrated Circuits (ICs) (Mamun and Alam, 2022). A study on Fiber Optic Gyroscopes (FOG) highlights the importance of considering temperature and humidity as sensitive stress factors in developing acceleration models for high-precision FOGs (Wang and Tang, 2020).

For a more precise expression, $T_{eff_{Peck}}$ and $RH_{eff_{Peck}}$ were introduced in the latest research by Damo et al. (2023):

$$T_{eff_{Peck}} = \frac{-E_a}{R_1\ \log_e(\frac{\sum_i G_i.(RH_i)^n.e^{(\frac{-E_a}{R_1.T_i})}(\delta t)_i}{\sum_i G_i.(RH_i)^n.(\delta t)_i})} \tag{12}$$

$$RH_{eff_{Peck}} = antilog\left(\frac{\log(\sum_i G_i.(RH_i)^n.e^{(\frac{-E_a}{R_1.T_i})}.(\delta t)_i) - \log(\sum_i G_i.e^{(\frac{-E_a}{R_1.T_i})}.(\delta t_i))}{n}\right) \tag{13}$$

Therefore, the accelerated factor for the combined effect of temperature, irradiance, cyclic temperature and Peck's relative humidity $AF_{T,G,\Delta T,RH_{Peck}}$ is provided by Eq. (14).

$$AF_{T,G,\Delta T,RH_{Peck}} = \frac{G_{lab}}{G_{site}}\left(\frac{\Delta T_{lab}}{\Delta T_{site}}\right)^{\alpha}.\left(\frac{RH_{lab}}{RH_{site}}\right)^{n}.e^{\frac{-E_a}{R_1}.(\frac{1}{T_{lab}} - \frac{1}{T_{site}})} \tag{14}$$

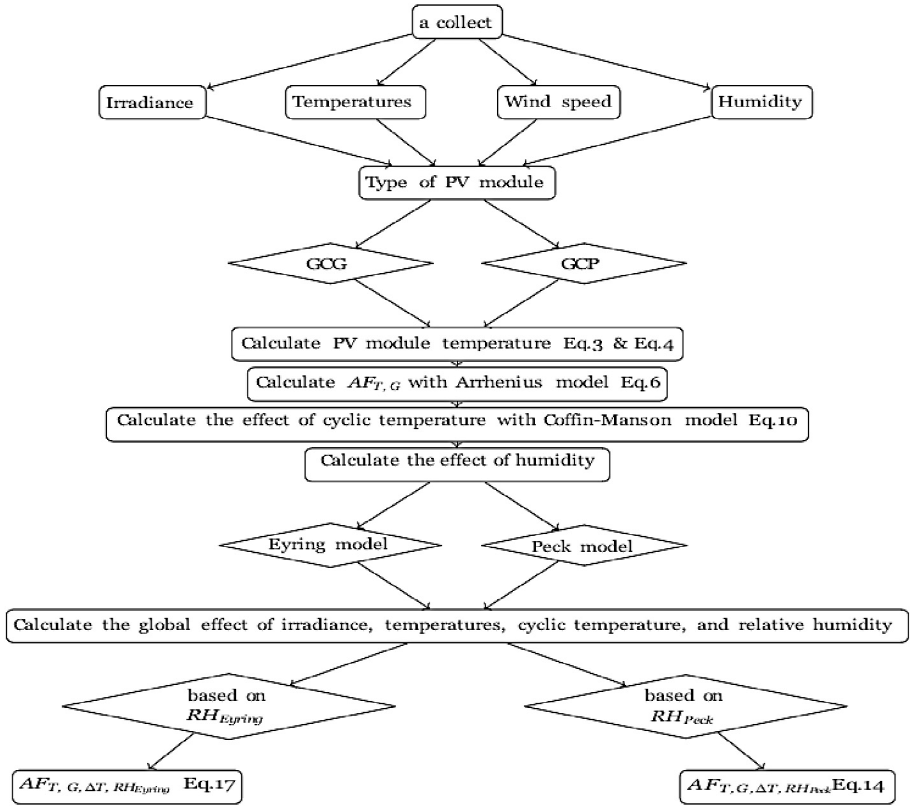


**Fig. 3.** Flowchart of the calculation process for Acceleration Factor (AF).

### *2.4.2. Eyring model*

The Eyring model is utilized in PV degradation studies to understand the impact of humidity on the reliability of PV modules. Research indicates that moisture ingress significantly affects the reliability of PV modules, participating in multiple degradation pathways (Nalin Venkat et al., 2023). Studies in humid and hot climates show an average degradation rate of 1.18%/year, with corrosion being a primary degradation mode (Marwaha and Ghosh, 2022). More on, investigations emphasize the importance of understanding the degradation of PV cells due to factors like humidity and temperature, which are major contributors to PV module degradation (Li et al., 2019). Accelerated degradation testing (ADT) techniques, such as Step-Stress ADT, can provide statistically rigorous predictions of lifetime and degradation rates under thermal-humidity stress conditions, utilizing the Eyring model for analysis (Yousuf et al., 2021). These findings highlight the significance of considering humidity within the Eyring model when studying PV degradation pathways.

$$T_{eff_{Eyring}} = \frac{-E_a}{R_1 \log_e\left(\frac{\sum_i G_i.e^{\left(\frac{-E_a}{R_1.T_i}-\frac{\beta}{R_1.RH_i}\right)}(\delta t)_i}{\sum_i G_i.e^{\left(\frac{-\beta}{R_1.RH_i}\right)}.(\delta t)_i}\right)} \tag{15}$$

$$RH_{eff_{Eyring}} = \frac{-\beta}{\log_e\left(\frac{\sum_i G_i.e^{\left(\frac{-E_a}{R_1.T_i}-\frac{\beta}{RH_i}\right)}.(\delta t)_i}{\sum_i G_i.e^{\frac{-E_a}{R_1.T_i}}.(\delta t)_i}\right)} \tag{16}$$

Eq. (17), therefore, introduces the accelerated factor for the combined influence of temperature, irradiance, cyclic temperature, and Eyrings's relative humidity $AF_{T,G,\Delta T,RH_{Eyring}}$.

$$AF_{T,G,\Delta T,Rh_{Eyring}} = \frac{G_{lab}}{G_{site}}.\left(\frac{\Delta T_{lab}}{\Delta T_{site}}\right)^{\alpha}.e^{\left(\frac{-E_a}{R_1}.\left(\frac{1}{T_{lab}}-\frac{1}{T_{site}}\right)-\beta.\left(\frac{1}{RH_{lab}}-\frac{1}{RH_{site}}\right)\right)} \tag{17}$$

Fig. 3 summarizes the process for calculating the AFs at any location globally, either by using relative humidity in the Peck model Eq. (14) or the Eyring model Eq. (17). Both models are employed to evaluate the combined impact of temperature and relative humidity on the aging of PV panels, which is critical in natural environments where these factors significantly contribute to degradation. According to the literature, the Eyring model is often preferred for describing the relationship between lifetime and temperature under single-stress conditions, while the Peck model accounts for the influence of relative humidity. This combined approach provides a more comprehensive understanding when both environmental factors are considered. The generalized Eyring model offers deeper insights into accelerated degradation mechanisms under joint-stress conditions, as demonstrated in various industrial applications, by integrating the effects of temperature and humidity into a unified framework (Wang et al., 2013).

## 3. Application of the AFs to the Oued El Keberit Solar plant

### *3.1. Oued El Keberit solar plant*

In this study, we applied the preceding equations based on the combined models to quantify the degradation mechanisms of one of Algeria's most prominent solar power plants. The Oued El Keberit Solar Power Plant (see Fig. 4), located in Souk Ahras, Algeria, at latitude 35.93 and longitude 7.86, is situated in a Mediterranean climate (Csa) according to the Köppen classification, where 'C' represents a warm temperate climate, 's' indicates dry summers, and 'a' refers to hot summer temperatures (Anon, 2024), and corresponds to a renewable energy project completed in 2016 with a capacity of 15 MWp. This PV power station utilizes polycrystalline silicon modules mounted on fixed support structures, and it includes 500 kW inverters and 0.4/30 kV, 1 MW transformers, connected to a 30 kV evacuation substation.


**Fig. 4.** Oued El Keberit solar power plant.

### 3.2. Climatic data

Fig. 5 depicts the hourly fluctuations in the climate data, encompassing measurements of irradiance, temperature, wind speed, and humidity, recorded every 15 min during a typical day for each season by the weather station of the power plant: winter (01/01/2022), spring (04/01/2022), summer (07/01/2022), and autumn (10/07/2024). The climate data used in this study was obtained from the meteorological station at the power plant. In summer, the intensity of sunlight reaches its highest point around midday because of the longer duration of daylight and the steeper angle at which the sun shines. In spring and autumn, the intensity is moderate, while in winter, it is at its lowest. The temperature data indicates that the highest values occur during summer, reaching their peak in the early afternoon. In contrast, spring and autumn see moderate temperatures with obvious changes throughout the day, while winter has the lowest temperatures with little fluctuations. The wind speed reaches its peak during the spring season, which signifies the transition between seasons. It decreases during summer, suggesting more tranquil weather conditions. In autumn and winter, the wind speed is moderate, with autumn seeing somewhat greater speeds compared to winter. Humidity reaches its peak during winter as the colder air has a reduced capacity to hold moisture. It is moderate during spring and autumn, and lowest during summer when the warmer air can hold more moisture, resulting in drier circumstances. The observed fluctuations in climate data across different seasons are in line with anticipated changes that occur throughout the year. These changes are influenced by factors such as the angle of the sun, air circulation, and the transitions between seasons.

For a more comprehensive climatic analysis, Fig. 6 illustrates the fluctuations in the four selected climatic data variables. During the winter season, the amount of irradiance typically hovers around 200 W/m$^2$ with minimal fluctuations. However, in spring and summer, the median irradiance increases to approximately 300–400 W/m$^2$, indicating greater variability and occasionally higher values. The irradiance in autumn is somewhat less than 400 W/m$^2$ with decreased fluctuation. The temperature throughout winter is around a median of 15 °C, decreases slightly during spring, reaches its highest point close to 30 °C during summer with notable fluctuations, and then descends to approximately 20 °C in autumn. The wind speed exhibits low medians and variability during the winter and summer seasons, while it demonstrates greater medians and a wider range during spring and autumn seasons. Notably, there are significant outliers throughout spring and summer. The wind speed exhibits low medians and variability during the winter and summer seasons, while it demonstrates greater medians and a wider range during the spring and autumn seasons. Notably, there are significant outliers throughout the spring and summer. The humidity remains at an average of over 40% during the winter and fall seasons. A noteworthy peak is observed in winter mornings, particularly around 8:30 am, owing to unique local weather patterns where passing clouds momentarily increase humidity levels before dissipating. This behavior, typical of the Mediterranean climate, can lead to sharp, short-lived humidity spikes, particularly in cooler conditions. Similarly, these early mornings can experience intermittent cloud cover, leading to slight but sudden changes in solar intensity. As the climate warms up in spring, the temperatures climb and humidity gradually decreases during spring and drops to roughly 25% during summer, with occasional higher values during winter and autumn. Different visualizations show the unique seasonal patterns and variations according to meteorological factors.

### 3.3. PV panel characteristics

The Oued Keberit PV power plant consists of 15 subfields, each having a capacity of 1 MWp, resulting in a total capacity of 15 MWp. The plant consists of 15 subfields, each containing 4004 panels. In total, there are 60,060 panels over the entire facility. The PV panels used in this installation are polycrystalline modules shown in Fig. 7 manufactured by YINGLI SOLAR, a Chinese company. More precisely, the model employed is the Yingli YL250P-29b. The main electrical characteristics of these panels are provided in Table 1.

### 3.4. Results and discussion

The provided Table 2 displays the AFs of PV panels during the four seasons. In winter, the AFs vary between 2819 and 3870 for an activation energy of 34 kJ/mol, with factors exhibiting higher values for increased activation energy. In spring, the AFs corresponding to an activation energy of 34 kJ/mol range from 7713 to 82,983. These AFs are more pronounced than in winter. On summer days, the values

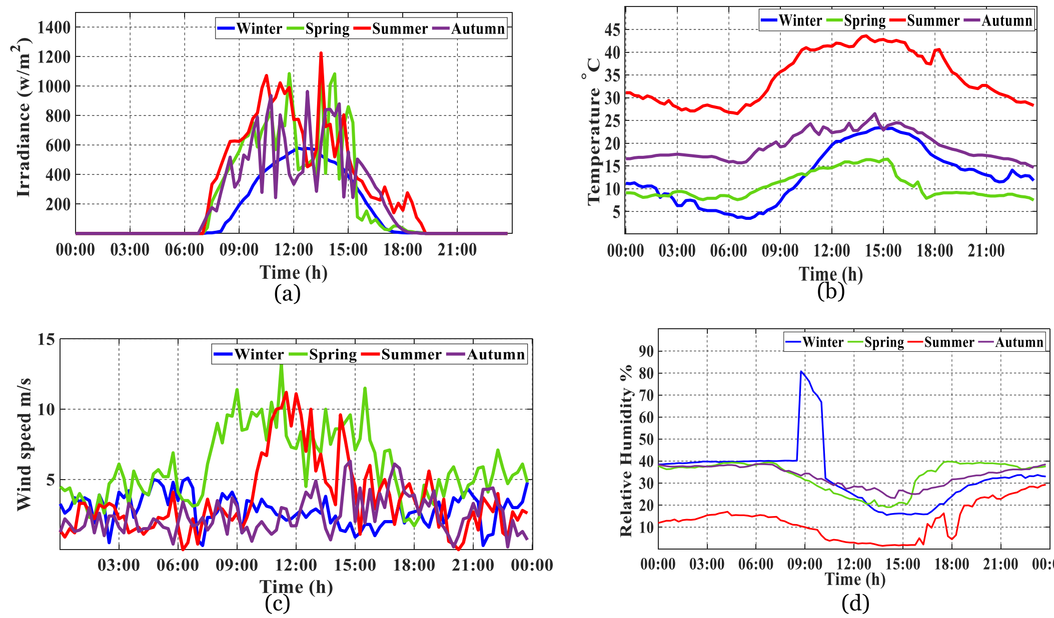


**Fig. 5.** Hourly climatic changes presentation (a) irradiance, (b) temperature, (c) wind speed, (d) humidity, for winter (01/01/2022), spring (04/01/2022), summer (08/01/2022), and autumn (10/01/2022).

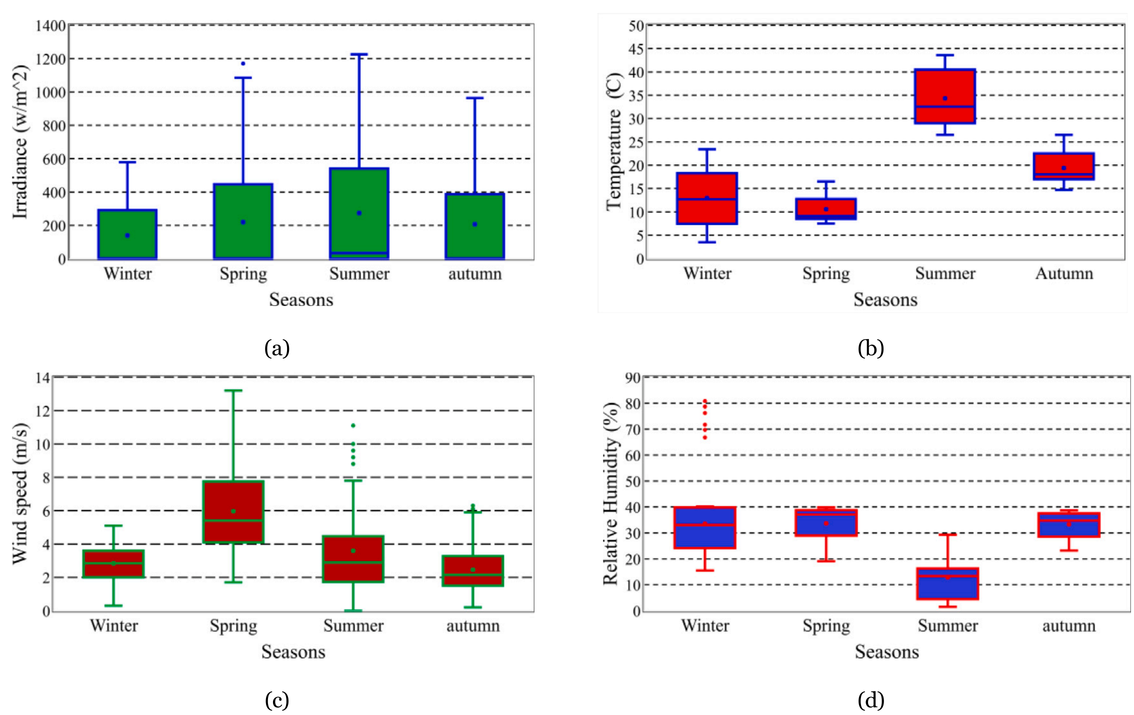


**Fig. 6.** Analysis of the hourly climatic changes for the four seasons (a): irradiance, (b): temperature, (c): wind speed, (d): humidity.

**Table 1**
PV Panel characteristics.

| Parameters | Values |
|---|---|
| STC Power rating [W] | 250.5 |
| Number of cells | 60 |
| Maximum power voltage $V_{mp}$ [V] | 30.4 |
| Maximum power current $I_{mp}$ [A] | 8.24 |
| Open-circuit voltage $V_{oc}$ [V] | 38.4 |
| Short-circuit current $I_{sc}$ [A] | 8.79 |

for 34 kJ/mol range from 181,794 to 514,457,721, indicating significantly higher AFs. These findings imply that factors such as higher temperatures, reduced humidity, fewer temperature fluctuations, and increased irradiance contribute to longer-lasting solar panels. These results are consistent with the earlier works in the literature including the prior research conducted by Damo et al. (2023) (Damo et al., 2023). During autumn, the AFs for 34 kJ/mol range from 3300 to 28,105. These observed values in autumn are lower than those recorded in spring and summer, yet higher than those in winter. This pattern indicates a moderate influence of autumnal weather conditions on the

**Table 2**
Accelerated factor of the PV Panel for the four seasons.

| $E_a$ [Kj/mol] | $AF_T$ | $AF_{T,G}$ | $AF_{T,RH_{Eyring}}$ | $AF_{T,RH_{Peck}}$ | $AF_{T,\Delta T}$ | | | $AF_{T,G,\Delta T,RH_{Eyring}}$ | | | $AF_{T,G,\Delta T,RH_{Peck}}$ | | |
|---|---|---|---|---|---|---|---|---|---|---|---|---|---|
| | | | | | $\alpha_1$ | $\alpha_2$ | $\alpha_3$ | $\alpha_1$ | $\alpha_2$ | $\alpha_3$ | $\alpha_1$ | $\alpha_2$ | $\alpha_3$ |
| **Winter day: 01/01/2022** | | | | | | | | | | | | | |
| 34 | 7.104 | 51.0094 | 253.5968 | 191.6355 | 14.5535 | 14.8691 | 15.0987 | 3730.4313 | 3811.3286 | 3870.1843 | 2818.9755 | 2880.1072 | 2924.5827 |
| 42 | 11.1397 | 79.9878 | 486.5726 | 349.2158 | 22.8213 | 23.3162 | 23.6762 | 7157.5259 | 7312.7424 | 7425.668 | 5136.9943 | 5248.3941 | 5329.4413 |
| 50.1 | 17.5067 | 125.7051 | 936.7584 | 637.2406 | 35.8649 | 36.6426 | 37.2085 | 13 779.7977 | 14 078.6234 | 14 296.0297 | 9373.8653 | 9577.1449 | 9725.038 |
| **Spring day: 04/01/2022** | | | | | | | | | | | | | |
| 34 | 7.0748 | 32.2455 | 7803.7371 | 755.9044 | 15.8381 | 16.2245 | 16.5063 | 79 623.5794 | 81 566.4129 | 82 983.108 | 7712.6908 | 7900.8822 | 8038.1095 |
| 42 | 11.0298 | 50.2715 | 13 959.0745 | 1237.7789 | 24.6919 | 25.2944 | 25.7337 | 142 428.103 | 145 903.3813 | 148 437.52 | 12 629.3835 | 12 937.5433 | 13 162.2504 |
| 50.1 | 17.1909 | 78.3521 | 24 981.8825 | 2024.3139 | 38.4843 | 39.4233 | 40.108 | 254 896.7076 | 261 116.2455 | 265 651.4715 | 20 654.6065 | 21 158.5836 | 21 526.0787 |
| **Summer day: 07/01/2022** | | | | | | | | | | | | | |
| 34 | 2.2834 | 8.3449 | 64 686 234.0553 | 23 741.8336 | 4.7841 | 4.8911 | 4.969 | 495 309 605.6252 | 506 390 984.132 | 514 457 720.8768 | 181 793.8298 | 185 861.0359 | 188 821.7759 |
| 42 | 2.7302 | 9.9779 | 163 406 175.5375 | 32 426.3929 | 5.7203 | 5.8483 | 5.9415 | 830 125 827.1858 | 848 697 925.1117 | 862217563.0047 | 248 292.455 | 253 847.4102 | 257 891.1635 |
| 50.1 | 3.2541 | 11.8927 | 302 109 031.7644 | 44 239.3933 | 6.818 | 6.9706 | 7.0816 | 1 401 679 772.5693 | 1 433 039 035.3996 | 1 455 867 144.5205 | 338 745.8979 | 346 324.5345 | 351 841.4353 |
| **Autumn day: 10/01/2022** | | | | | | | | | | | | | |
| 34 | 4.8184 | 23.3381 | 2548.2475 | 311.5019 | 10.5404 | 10.7901 | 10.9721 | 26 999.3482 | 27 639.0266 | 28 105.1978 | 3300.4438 | 3378.6391 | 3435.6246 |
| 42 | 6.8634 | 33.243 | 3837.2168 | 452.291 | 15.0138 | 15.3695 | 15.6287 | 40 656.3143 | 41 619.5585 | 42 321.5312 | 4792.1408 | 4905.678 | 4988.4192 |
| 50.1 | 9.7637 | 47.2906 | 5763.4657 | 655.4281 | 21.3582 | 21.8642 | 22.233 | 61 065.4248 | 62 512.2091 | 63 566.5659 | 6944.4317 | 7108.9618 | 7228.8644 |

**Fig. 7.** PV array.

performance of PV panels. It is crucial to consider seasonal environmental conditions when assessing the durability and performance of PV panels, as highlighted by the data. Due to the variability of AFs across many parameters, employing advanced modeling techniques is necessary to accurately forecast the lifespan of PV panels under specific local conditions. To optimize PV panel design and maintenance and increase their longevity and efficacy, a comprehensive approach is required.

Fig. 8 compares the AFs for each studied parameter across the four seasons. The highest values of $AF_T$ and $AF_G$ are observed in the winter season, indicating that these parameters have minimal impact on the PV panels during this time. Conversely, the highest value of $AF_{dT}$ occurs during the spring season, suggesting that temperatures are more stable in spring and thus have a lesser effect on the PV panels. The summer season, characterized by low humidity, exhibits a higher $AF_{RH}$ indicating that relative humidity during summer does not impact the PV panels compared to other seasons. In plus, the effects of increasing activation energies (Ea) on the accelerated weathering parameters: 34 kJ/mol, 42 kJ/mol, and 50.1 kJ/mol are also illustrated. Generally, higher $E_a$ values correspond to slower degradation rates under lower environmental stress factors. However, when exposed to elevated humidity levels, the AFs can increase significantly, indicating a more pronounced degradation effect under these conditions.

Fig. 9 displays clear and identifiable patterns that vary with the seasons. In winter, humidity stands out as the foremost factor degrading PV panels, followed by cyclic temperature fluctuations, whereas direct temperature and irradiance exhibit comparatively minor effects. During spring, humidity significantly influences panels, with irradiance as a secondary factor, and direct temperature and cyclic temperature ranking as the least impactful. In summer, panels are primarily affected by direct temperature and irradiance, while humidity and cyclic temperature play a minimal role. Autumn shows a pronounced impact of humidity on panels, followed by irradiance and temperature, with cyclic temperature fluctuations having minimal effect as shown in Fig. 9.

Various strategies to mitigate the impact of relative humidity on PV systems have been extensively investigated in the literature. Below, we outline several notable approaches:

- Phase Change Materials (PCMs): Incorporating PCMs into PV system designs can help regulate temperature fluctuations caused by humidity. PCMs absorb the excess heat during temperature rises, which aids in maintaining optimal humidity levels around the panels (Nabil and Mansour, 2024).
- Cooling Systems: Implementing cooling systems, such as evaporative cooling, is a practical solution, particularly in humid environments. These systems lower the temperature of PV panels, thereby enhancing their efficiency and performance. Abdelwahab et al. (2024) demonstrated that a dual-cooling approach significantly reduced both the front and back temperatures of PV modules.
- Dew-Point Evaporative Cooling (DPEC): This advanced method reduces the inlet air temperature below the wet-bulb temperature, making it highly effective for cooling PV panels. By boosting cooling efficiency, DPEC also facilitates better humidity management positioning it as a promising technology for PV cooling systems (Yang et al., 2024).
- Water Recovery Systems: Khalid et al. (2023) proposed a sustainable approach utilizing water recovery systems to manage water consumption during PV panel cleaning. This method is particularly beneficial in humid regions where water scarcity is a concern.
- Surface Treatments: The application of hydrophobic coatings to backsheets minimizes moisture absorption. These treatments create a barrier that prevents water from penetrating the material, thereby preserving its insulating properties (Anagha et al., 2023).

## 4. Conclusion and perspectives

This paper presents innovative theoretical equations that were developed to examine the collective impact of irradiance, temperature, humidity, and cyclic temperature on the acceleration factors of PV panels, marking the first comprehensive analysis of this kind. The theoretical equations used in this study combine various well-established models, such as the Arrhenius model for temperature and irradiance, the Eyring and Peck models for humidity, and the Coffin–Manson model for cyclic temperature changes. These equations offer general applicability across different global locations, as they consider temperature and its fluctuations, wind speed, irradiance, and humidity.

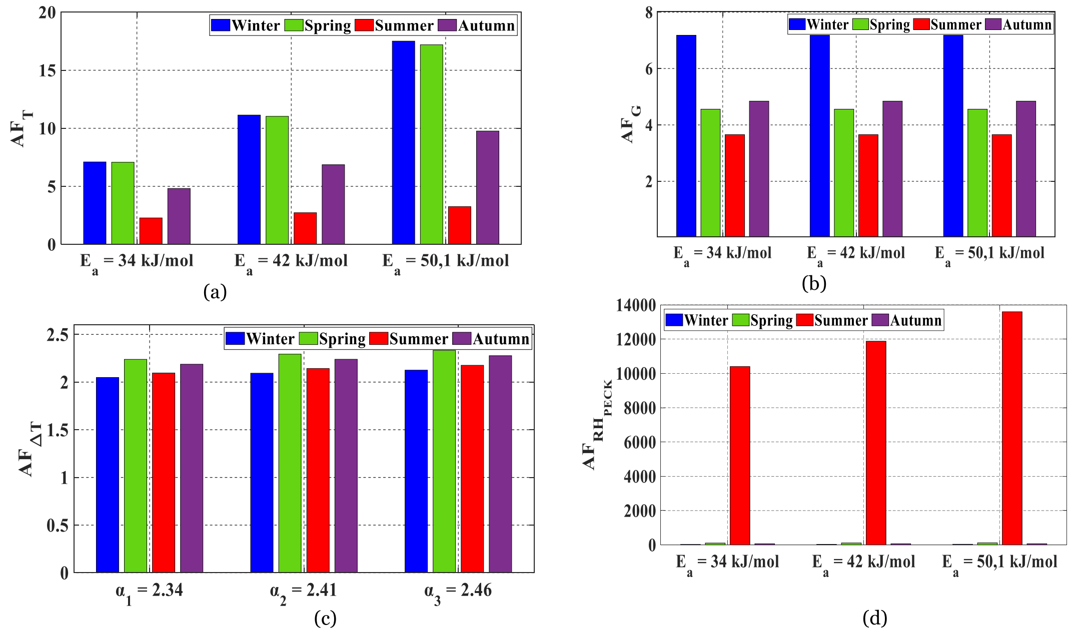


**Fig. 8.** Analysis of the AFs for the four seasons: (a): AFs of temperature, (b): AFs of irradiance, (c): AFs of cyclic temperature, (d): AFs of humidity based on Peck model.

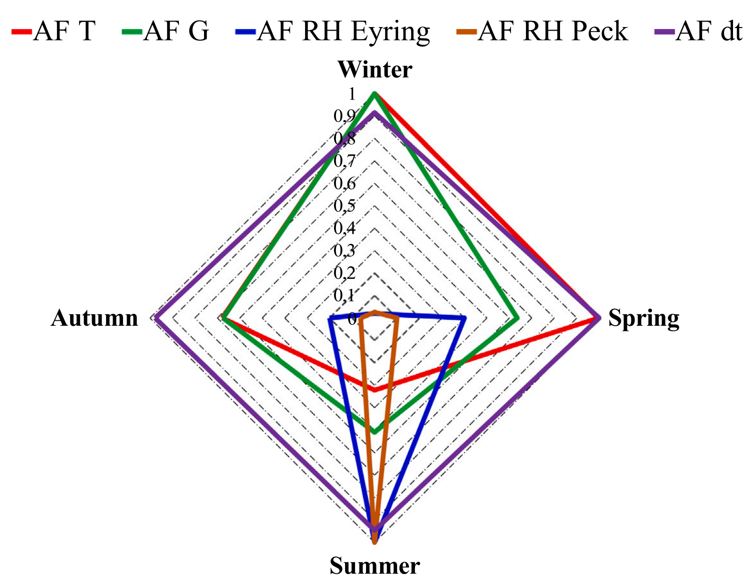


**Fig. 9.** Comparison between the AFs of the four seasons.

This approach results in more accurate predictions compared to those commonly found in the literature.

The derived equations were utilized to analyze the Oued El Keberit solar power plant, which is widely recognized as one of the most prominent solar facilities in Algeria. To conduct the investigation, one day was selected from each season (winter, spring, summer, and autumn) in order to evaluate the impact of climatic variables on the deterioration of PV panels. The values of $E_a$ (34 kJ/mol, 42 kJ/mol, and 50.1 kJ/mol) were considered in the analysis, showing that there was a direct relationship between higher activation energy and increased acceleration factors, indicating a greater sensitivity to environmental variables. Also, the three values ($\alpha_1 = 2.34$, $\alpha_2 = 2.41$, and $\alpha_3 = 2.46$) of the constant $\alpha$ based on product characteristics were taken into account . The findings revealed that during winter, humidity exerted the greatest influence on the performance of the PV panels, while temperature irradiance and cyclic temperature had a comparatively less impact with AFs during this season being 64 times lower than in summer ($AF_{winter} = 1.55\%\ AF_{summer}$). In spring, PV panels are susceptible to the influence of both humidity and irradiance, and the AFs are 24 times lower ($AF_{spring} = 4.24\%\ AF_{summer}$). In autumn, humidity once again has a notable impact, while the fluctuating temperature has a minor influence, and the AFs are 55 times lower ($AF_{autumn} = 1.81\%\ AF_{summer}$). This indicates that PV panels would degrade more rapidly in winter, where the lower AF values reflect accelerated degradation due to higher relative humidity. Conversely, the higher AF values in summer suggest a slower degradation rate. These observations suggest that conditions such as lower humidity, higher temperatures, increased irradiance, and reduced temperature fluctuations contribute to a longer lifespan for solar panels. Based on these data, it can be inferred that humidity is the primary element that contributes to the deterioration of the PV panels. Various strategies from the literature have been provided to reduce the impact of relative humidity on PV systems. PCMs help stabilize temperatures by absorbing excess heat, thus controlling humidity levels. Cooling systems, like evaporative cooling, improve PV efficiency, especially in humid environments. DPEC further enhances cooling efficiency by reducing air temperature below the wet-bulb level. Water recovery systems promote sustainable water use in PV cleaning, and hydrophobic surface treatments protect PV backsheets by preventing moisture absorption and maintaining insulation performance.

Future studies should emphasize comprehensive economic analyses that acknowledge the outstanding potential of PV energy while also meticulously assessing the long-term cost implications of panel degradation. By elucidating the financial impacts associated with various degradation rates, investors and policymakers can make informed decisions that optimize the benefits of solar energy investments. Addressing these degradation factors in advance will not only enhance the sustainability of PV systems, but also ensure their continued effectiveness as a fundamental aspect of renewable energy.

## CRediT authorship contribution statement

**Meriem Farou:** Writing – review & editing, Writing – original draft, Visualization, Methodology, Conceptualization. **Abdelhak Djellad:** Validation, Supervision, Data curation. **Sofiane Chiheb:** Validation. **Hala Lalaymia:** Validation. **Badri Rekik:** Validation, Data curation. **Pierre-Olivier Logerais:** Validation.

## Declaration of competing interest

The authors declare that they have no known competing financial interests or personal relationships that could have appeared to influence the work reported in this paper.

## Acknowledgment

The authors express their sincere gratitude to Mrs. Wilhelmina LOGERAIS, a native English speaker, for her valuable contribution to proofreading this article. Her expertise and assistance in refining the language and clarity of the manuscript are greatly appreciated.

## Data availability

The data that has been used is confidential.

## References

Abdelwahab, T.A.M., Fodah, A.E.M., Ali, K.A.M., Osman, Y.K.O.T., Abuhussein, M.F.A., Abd El-wahhab, G.G., 2024. Innovative cooling technique to improve the performance of photovoltaic panels. Appl. Therm. Eng. 248, 123316. http://dx.doi.org/10.1016/j.applthermaleng.2024.123316, URL https://linkinghub.elsevier.com/retrieve/pii/S1359431124009840.

Alavi, O., Kaaya, I., De Jong, R., De Ceuninck, W., Daenen, M., 2024. Assessing the impact of PV panel climate-based degradation rates on inverter reliability in grid-connected solar energy systems. Heliyon 10 (3), e25839. http://dx.doi.org/10.1016/j.heliyon.2024.e25839, URL https://linkinghub.elsevier.com/retrieve/pii/S240584402401870X.

Anagha, E., Narasimhan, K., Kulkarni, S., Shiradkar, N., 2023. Humidity-induced electrical conduction in fluropolymer-based photovoltaic backsheets. Sol. Energy 263, 111947. http://dx.doi.org/10.1016/j.solener.2023.111947, URL https://linkinghub.elsevier.com/retrieve/pii/S0038092X23005807.

Anon, 2024. World maps of Köppen-Geiger climate classification, URL https://koeppen-geiger.vu-wien.ac.at/present.htm.

Bae, D., Faasse, G.M., Smith, W.A., 2020. Hidden figures of photo-charging: A thermo-electrochemical approach for a solar-rechargeable redox flow cell system. Sustain. Energy Fuels 4 (6), 2650–2655. http://dx.doi.org/10.1039/D0SE00348D, URL https://xlink.rsc.org/?DOI=D0SE00348D.

Bala Subramaniyan, A., Pan, R., Kuitche, J., TamizhMani, G., 2018. Quantification of environmental effects on PV module degradation: A physics-based data-driven modeling method. IEEE J. Photovolt. 8 (5), 1289–1296. http://dx.doi.org/10.1109/JPHOTOV.2018.2850527, URL https://ieeexplore.ieee.org/document/8410667/.

Briand, A., Leybros, A., Doucet, O., Ruiz, J.-C., Fontaine-Giraud, P., Liotaud, L., Grandjean, A., 2023. Versatility assessment of supercritical CO2 delamination for photovoltaic modules with ethylene-vinyl acetate, polyolefin or ethylene methacrylic acid ionomer as encapsulating polymer. J. Clean. Prod. 410, 137292. http://dx.doi.org/10.1016/j.jclepro.2023.137292, URL https://linkinghub.elsevier.com/retrieve/pii/S0959652623014506.

Burlafinger, K., 2020. Development of a High Irradiance Setup for Precisely Controlled Accelerated Photo-Degradation of Organic Solar Cells (Ph.D. thesis). Friedrich-Alexander-Universität Erlangen-Nürnberg (FAU).

Capo-Chichi, M.M., Madogni, V.I., Kouchadé, C.A., Hounkpatin, G.F., Agbomahéna, M., Kounouhewa, B., 2022. Effects of damp-heat on shunt, series resistances and fill factor into crystalline silicon photovoltaic solar modules in tropical zone. Phys. Sci. Int. J. 1–16. http://dx.doi.org/10.9734/psij/2022/v26i6747, URL https://journalpsij.com/index.php/PSIJ/article/view/747.

Chen, C., Chen, H., Hsueh, C., Chang, M., 2014. Behavior of light-induced degradation for temperature cycling test. In: 2014 IEEE 40th Photovoltaic Specialist Conference. PVSC, IEEE, pp. 3177–3181.

Çolak, A.B., 2022. Analysis of the effect of arrhenius activation energy and temperature dependent viscosity on non-Newtonian maxwell nanofluid bio-convective flow with partial slip by artificial intelligence approach. Chem. Thermodyn. Therm. Anal. 6, 100039. http://dx.doi.org/10.1016/j.ctta.2022.100039, URL https://linkinghub.elsevier.com/retrieve/pii/S2667312622000062.

Cronin, A., Pulver, S., Cormode, D., Jordan, D., Kurtz, S., Smith, R., 2014. Measuring degradation rates of PV systems without irradiance data. Prog. Photovolt., Res. Appl. 22 (8), 851–862.

Dalton, E., Ren, G., Punch, J., Collins, M.N., 2018. Accelerated temperature cycling induced strain and failure behaviour for BGA assemblies of third generation high Ag content Pb-free solder alloys. Mater. Des. 154, 184–191. http://dx.doi.org/10.1016/j.matdes.2018.05.030, URL https://linkinghub.elsevier.com/retrieve/pii/S0264127518304155.

Damo, U., Ozoegwu, C.G., Ogbonnaya, C., Maduabuchi, C., 2023. Effects of light, heat and relative humidity on the accelerated testing of photovoltaic degradation using Arrhenius model. Sol. Energy 250, 335–346. http://dx.doi.org/10.1016/j.solener.2023.01.002, URL https://linkinghub.elsevier.com/retrieve/pii/S0038092X23000026.

Doumane, R., Balistrou, M., Logerais, P.O., Riou, O., Durastanti, J.-F., Charki, A., 2015. A circuit-based approach to simulate the characteristics of a silicon photovoltaic module with aging. J. Sol. Energy Eng. 137 (2), 021020.

Dzurick, M., Potter, B., Holmgren, W.F., Simmons-Potter, K., 2019. Enhanced photovoltaic power model fidelity using on-site irradiance and degradation-informed performance input. In: 2019 IEEE 46th Photovoltaic Specialists Conference. PVSC, IEEE, pp. 1596–1600. http://dx.doi.org/10.1109/PVSC40753.2019.8980708, URL https://ieeexplore.ieee.org/document/8980708/.

Escobar, L.A., Meeker, W.Q., 2006. A review of accelerated test models. Statist. Sci. 21 (4), http://dx.doi.org/10.1214/088342306000000321, URL https://projecteuclid.org/journals/statistical-science/volume-21/issue-4/A-Review-of-Accelerated-Test-Models/10.1214/088342306000000321.full.

Feil, F., McGreer, M., Cordo, O., 2022. Photochemical aging and weathering of polymers—The basics.

Gopinath, M., Marimuthu, R., 2024. Experimental study of photovoltaic-thermoelectric generator with graphite sheet. Case Stud. Therm. Eng. 54, 103982. http://dx.doi.org/10.1016/j.csite.2024.103982, URL https://linkinghub.elsevier.com/retrieve/pii/S2214157X24000121.

Herrmann, W., 2010. How temperature cycling degrades photovoltaic-module performance. In: International Society Advancing an Interdisciplinary Approach to the Science and Application of Light. SPIE.

Hulkoff, T., 2009. Usage of highly accelerated stress test (HAST) in solar module ageing procedures.

Johnston, S., Xiao, C., Deceglie, M.G., Gaulding, A., Jiang, C.-S., Guthrey, H., Kern, D.B., Kroeger, G.F., Al-Jassim, M., Repins, I.L., 2022. Light-and elevated-temperature-induced degradation-affected silicon cells from a utility-scale photovoltaic system characterized by deep-level transient spectroscopy. IEEE J. Photovolt. 12 (3), 703–710.

Karas, J., Repins, I., Berger, K.A., Kubicek, B., Jiang, F., Zhang, D., Jaubert, J.-N., Cueli, A.B., Sample, T., Jaeckel, B., et al., 2023. Results from an International Interlaboratory Study on Light-and Elevated Temperature-Induced Degradation (LETID) in Solar Modules. Tech. rep., National Renewable Energy Lab.(NREL), Golden, CO (United States).

Khalid, H.M., Rafique, Z., Muyeen, S., Raqeeb, A., Said, Z., Saidur, R., Sopian, K., 2023. Dust accumulation and aggregation on PV panels: An integrated survey on impacts, mathematical models, cleaning mechanisms, and possible sustainable solution. Sol. Energy 251, 261–285. http://dx.doi.org/10.1016/j.solener.2023.01.010, URL https://linkinghub.elsevier.com/retrieve/pii/S0038092X23000105.

Kidegho, G., Njoka, F., Muriithi, C., Kinyua, R., 2021. Evaluation of thermal interface materials in mediating PV cell temperature mismatch in PV–TEG power generation. Energy Rep. 7, 1636–1650. http://dx.doi.org/10.1016/j.egyr.2021.03.015, URL https://linkinghub.elsevier.com/retrieve/pii/S2352484721001840.

Koehl, M., Hoffmann, S., Wiesmeier, S., 2017. Evaluation of damp-heat testing of photovoltaic modules. Prog. Photovolt., Res. Appl. 25 (2), 175–183.

Kurtz, M.A., Alaniz, K., Taylor, L.M., Moreno-Reyes, A., Gilbert, J.L., 2024. Increasing temperature accelerates Ti-6Al-4V oxide degradation and selective dissolution: An arrhenius-based analysis. Acta Biomater. 178, 352–365. http://dx.doi.org/10.1016/j.actbio.2024.02.028, URL https://linkinghub.elsevier.com/retrieve/pii/S1742706124000990.

Kyranaki, N., Smith, A., Yendall, K., Hutt, D.A., Whalley, D.C., Gottschalg, R., Betts, T.R., 2022. Damp-heat induced degradation in photovoltaic modules manufactured with passivated emitter and rear contact solar cells. Prog. Photovolt., Res. Appl. 30 (9), 1061–1071. http://dx.doi.org/10.1002/pip.3556, URL https://onlinelibrary.wiley.com/doi/10.1002/pip.3556.

Li, H., Lv, F., Diao, H., Chen, X., Wang, W., 2019. Evaluation of temperature and humidity on PV module degradation-in field degradation analysis of crystalline silicon module. In: 2019 IEEE 46th Photovoltaic Specialists Conference. PVSC, IEEE, pp. 1986–1990.

Liu, C., Cui, Y., Wang, K., Wang, B., 2024. Fatigue life prediction and energy conversion efficiency evaluation of a photovoltaic-thermoelectric device subjected to time-varying thermal and wind hybrid loads. Int. J. Solids Struct. 293, 112741. http://dx.doi.org/10.1016/j.ijsolstr.2024.112741, URL https://linkinghub.elsevier.com/retrieve/pii/S0020768324000982.

Liu, Q., Shi, W., Chen, Z., Li, K., Liu, H., Li, S., 2019. Rubber accelerated ageing life prediction by Peck model considering initial hardness influence. Polym. Test. 80, 106132. http://dx.doi.org/10.1016/j.polymertesting.2019.106132, URL https://linkinghub.elsevier.com/retrieve/pii/S014294181930933X.

Lugt, P.M., 2023. On the use of the Arrhenius equation to describe the impact of temperature on grease life.

Mahdi, H.A., Leahy, P., Morrison, A., 2021. Predicting early EVA degradation in photovoltaic modules from short circuit current measurements. IEEE J. Photovolt. 11 (5), 1188–1196. http://dx.doi.org/10.1109/JPHOTOV.2021.3086455, URL https://ieeexplore.ieee.org/document/9461216/.

Mamun, M.A.Z., Alam, M.A., 2022. Reduced relative humidity (RH) enhances the corrosion-limited lifetime of self-heated IC: Peck's equation generalized. In: 2022 IEEE International Reliability Physics Symposium. IRPS, IEEE, pp. 8A–5.

Marwaha, S., Ghosh, K., 2022. Analytical modeling of diffusion of moisture in silicon photovoltaic module under damp heat testing condition. Silicon 14 (9), 4757–4766.

Mistry, D., Paul, B., Chanda, C.K., 2022. Security of load flow analysis with photovoltaic energy sources. In: Computational Advancement in Communication, Circuits and Systems: Proceedings of 3rd ICCACCS 2020. Springer, pp. 219–232.

Mohamed, B., Zambou, S., Zekeng, S.S., 2017. Influence of moisture on the operation of a mono-crystalline based silicon photovoltaic cell: A numerical study using SCAPS 1 d. arXiv preprint arXiv:1712.08117.

Nabil, T., Mansour, T.M., 2024. Enhancing photovoltaic panel efficiency with innovative cooling technologies: An experimental approach. Appl. Therm. Eng. 253, 123846. http://dx.doi.org/10.1016/j.applthermaleng.2024.123846, URL https://linkinghub.elsevier.com/retrieve/pii/S135943112401514X.

Nalin Venkat, S., Yu, X., Liu, J., Wegmueller, J., Jimenez, J.C., Barcelos, E.I., Aung, H.H., Li, X., Jaubert, J.-N., French, R.H., et al., 2023. Statistical analysis and degradation pathway modeling of photovoltaic minimodules with varied packaging strategies. Front. Energy Res. 11, 1127796.

Perez, A., Mar, L., Fuentes, F., Mendoza, P., Jimenez, G., Orchard, M., 2019. Performance of photovoltaic modules after an accelerated thermal cycling degradation test. In: Proc. Annu. Conf. PHM Soc., vol. 11, (1), pp. 1–9.

Pramanick, D., Kumar, J., 2024. Performance and degradation assessment of two different solar PV cell technologies in the remote region of eastern India. e-Prime - Adv. Electr. Eng. Electron. Energy 7, 100432. http://dx.doi.org/10.1016/j.prime.2024.100432, URL https://linkinghub.elsevier.com/retrieve/pii/S2772671124000147.

Sarma, N., Paul, A., Patgiri, B., 2024. Computational study of jeffrey hybrid nanofluid flow over on a non-uniformly heated permeable exponentially stretching surface with arrhenius activation energy and inclined magnetic field. Hybrid Adv. 6, 100194. http://dx.doi.org/10.1016/j.hybadv.2024.100194, URL https://linkinghub.elsevier.com/retrieve/pii/S2773207X24000551.

Segbefia, O.K., Sætre, T.O., 2022. Investigation of the temperature sensitivity of 20-years old field-aged photovoltaic panels affected by potential induced degradation. Energies 15 (11), 3865.

Shaik, H.M., Kabbani, A., Sheikh, A.M., Goh, K., Gupta, N., Umar, T., 2021. Measurement and validation of polysilicon photovoltaic module degradation rates over five years of field exposure in oman. AIMS Energy 9 (6).

Solís-Alemán, E.M., De La Casa, J., Romero-Fiances, I., Silva, J.P., Nofuentes, G., 2019. A study on the degradation rates and the linearity of the performance decline of various thin film PV technologies. Sol. Energy 188, 813–824. http://dx.doi.org/10.1016/j.solener.2019.06.067, URL https://linkinghub.elsevier.com/retrieve/pii/S0038092X19306413.

Talib, I.F., 2022. PV system multiple source single inverter. Int. J. Innov. Res. Comput. Sci. Technol. 111–124. http://dx.doi.org/10.55524/ijircst.2022.10.4.13, URL https://ijircst.org/DOC/13-pv-system-multiple-source-single-inverter.pdf.

Tawagi, E., Ung, T., Cheng, H.-L.M., Santerre, J.P., 2023. Arrhenius-model-based degradable oligourethane hydrogels for controlled growth factor release. Acta Biomater. 166, 167–186. http://dx.doi.org/10.1016/j.actbio.2023.05.024, URL https://linkinghub.elsevier.com/retrieve/pii/S1742706123002805.

Torlo, M., Balić, T., Damir, v., 2023. Renewable energy sources photovoltaic power plants and constructive solutions related to locality and climate. In: International Conference "New Technologies, Development and Applications". Springer, pp. 22–28.

Urban, T., Müller, M., Heitmann, J., 2022. Full analysis of series resistance components and their degradation in temperature cycling of PERC solar cells. In: AIP Conference Proceedings, vol. 2487, (1), AIP Publishing.

Wang, W.Y., Ma, X.B., Chang, S.H., Kang, R., 2013. A comparison of two accelerated degradation models with temperature and humidity as accelerating stresses. Appl. Mech. Mater. 300–301, 1162–1170. http://dx.doi.org/10.4028/www.scientific.net/AMM.300-301.1162, URL https://www.scientific.net/AMM.300-301.1162.

Wang, Y., Tang, Y., 2020. Statistical analysis of accelerated temperature cycling test based on Coffin-Manson model. Comm. Statist. Theory Methods 49 (15), 3663–3680. http://dx.doi.org/10.1080/03610926.2019.1702697, URL https://www.tandfonline.com/doi/full/10.1080/03610926.2019.1702697.

Xu, J., Tu, H.T.C., Masuda, A., Ohdaira, K., 2022. Effect of temperature and pre-annealing on the potential-induced degradation of silicon heterojunction photovoltaic modules. Japan. J. Appl. Phys. 61 (SC), SC1021.

Yang, C., Lin, J., Miksik, F., Miyazaki, T., Thu, K., 2024. Dew-point evaporative cooling of PV panels for improved performance. Appl. Therm. Eng. 236, 121695. http://dx.doi.org/10.1016/j.applthermaleng.2023.121695, URL https://linkinghub.elsevier.com/retrieve/pii/S1359431123017246.

Yao, W., Ling, Q., Dai, Q., Fang, S., Yang, C., Huang, L., Liu, X., Zhang, H., Zhang, J., Zhu, Y., et al., 2022. In situ microscopic observation of humidity-induced degradation in all-inorganic perovskite films. ACS Appl. Energy Mater. 5 (7), 8092–8102.

Yekinni, S., Asiata, I., Hakeem, O., Mubarak, L., 2023. Solar photovoltaic energy system. In: Dudem, B., Venkateswaran, V., Chandrasekhar, A. (Eds.), Nanogenerators and Self-Powered Systems. IntechOpen, http://dx.doi.org/10.5772/intechopen.108958, URL https://www.intechopen.com/chapters/85762.

Yousuf, H., Khokhar, M.Q., Zahid, M.A., Kim, J., Kim, Y., Cho, S.B., Cho, Y.H., Cho, E.-C., Yi, J., 2021. A review on degradation of silicon photovoltaic modules. New Renew. Energy 17 (1), 19–32.

Zang, J., Qing, M., Chi, Y., Chi, Y., 2023. Predicting quality of the whole egg powder during storage: based on arrhenius and radial basis function model. J. Food Comp. Anal. 124, 105666. http://dx.doi.org/10.1016/j.jfca.2023.105666, URL https://linkinghub.elsevier.com/retrieve/pii/S0889157523005409.

Zhao, X., Liu, T., Burlingame, Q.C., Liu, T., Holley, R., Cheng, G., Yao, N., Gao, F., Loo, Y.-L., 2022. Accelerated aging of all-inorganic, interface-stabilized perovskite solar cells. Science 377 (6603), 307–310. http://dx.doi.org/10.1126/science.abn5679, URL https://www.science.org/doi/10.1126/science.abn5679.